Available online at www.sciencedirect.com
ScienceDirect
International Journal of Mass Spectrometry 259 (2007) 184–196
International Journal of Mass Spectrometry
www.elsevier.com/locate/ijms

Characterization of neurohistone variants and post-translational modifications by electron capture dissociation mass spectrometry

Benjamin A. Garcia [a], Nertila Siuti [b], C. Eric Thomas [b], Craig A. Mizzen [a,d], Neil L. Kelleher [a,b,c,*]

[a] *Institute for Genomic Biology, University of Illinois at Urbana-Champaign, Urbana, IL 61801, United States*
[b] *Department of Chemistry, University of Illinois at Urbana-Champaign, Urbana, IL 61801, United States*
[c] *The Center for Top Down Proteomics, University of Illinois at Urbana-Champaign, Urbana, IL 61801, United States*
[d] *Department of Cell and Developmental Biology, University of Illinois at Urbana-Champaign, Urbana, IL 61801, United States*

Received 26 May 2006; received in revised form 27 July 2006; accepted 28 July 2006

Dedicated to Professor Donald F. Hunt on the occasion of his 65th birthday, and in recognition and admiration of his many significant contributions to the advancement of biological mass spectrometry.

Abstract

Post-translational modifications (PTMs) of histones are intimately involved in chromatin structure and thus have roles in cellular processes through their impact on gene activation or repression. At the forefront in histone PTM analysis are mass spectrometry-based techniques, which have capabilities to produce improved views of processes affected by chromatin remodeling via histone modifications. In this report, we take the first mass spectrometric look at histone variant expression and post-translational modifications from histones isolated from rat brain tissue. Analyses of whole rat brain identified specific histone H2A and H2B gene family members and several H4 and H3 post-translational modification sites by electron capture dissociation (ECD) mass spectrometry. We subsequently compared these results to selected rat brain regions. Major differences in the expression profiles of H2A and H2B gene family members or in the post-translational modifications on histone H4 were not observed from the different brain regions using a Top Down approach. However, "Middle Down" mass spectrometry facilitating improved characterization of the histone H3 tail (1–50 residues), revealed an enrichment of trimethylation on Lys9 from cerebellum tissue compared to H3 extracted from whole brain, cerebral cortex or hypothalamus tissue. We forward this study in honor of Professor Donald F. Hunt, whose pioneering efforts in protein and PTM analyses have spawned new eras and numerous careers, many exemplified in this special issue.
Published by Elsevier B.V.

Keywords: Histone; Brain; Post-translational modification; Mass spectrometry; Electron capture dissociation (ECD)

1. Introduction

Genetic information in the eukaryotic nucleus is packaged into the fundamental unit of chromatin, the nucleosome, largely through association with histones. This histone-DNA complex consists of a protein octamer composed of two copies each of histones H2A, H2B, H3 and H4, around which approximately 147 bp of DNA are wrapped [1,2]. This basic repeating unit of chromatin is further compacted and folded into a fiber, as adjacent nucleosomes are linked by another complex consisting of histone H1 and linker DNA. Once regarded as merely static structural proteins needed to create the chromatin fiber, recent research has revealed histone proteins to be highly dynamic and intricately involved in the regulation of gene expression during several key cellular events. At the center of the regulatory process are the vast amounts of post-translational modifications (PTMs) that have been described to occur on histones and are linked to distinct cellular processes [3–5]. Core histones are known to be highly modified through lysine acetylation or methylation, and to a lesser extent by lysine ubiquitination, arginine methylation, and serine or threonine phosphorylation. These modifications are largely found on the N-terminal histone tails that protrude from the nucleosome.

* Corresponding author at: 600 S. Matthews Avenue., 53 Roger Adams Laboratory, Urbana, IL 61801, United States. Tel.: +1 217 244 3927.
E-mail address: Kelleher@scs.uiuc.edu (N.L. Kelleher).

1387-3806/$ – see front matter. Published by Elsevier B.V.
doi:10.1016/j.ijms.2006.07.022

Chromatin is generally categorized into two biologically and physically distinct forms: euchromatin, or open chromatin, that is transcriptionally permissive and heterochromatin, which is mostly transcriptionally silenced. These two different states of chromatin have been associated with specific histone PTMs, hence, these modifications have been postulated to form a "Histone Code" that is read by other nuclear proteins and directs cellular physiology in an epigenetic fashion [6,7]. Formally, the "Histone Code" hypothesis states that modifications or combinations of modifications on distinct histone residues act as a binding platform to recruit "effector" proteins which lead to gene activation or repression. Examples of this process include the proteins Heterochromatin protein 1 (HP1) and Polycomb which bind methylated Lys9 and methylated Lys27 on histone H3 and lead to gene silencing and formation of heterochromatin [8,9]. Other modifications that are linked to gene activation include Lys9 acetylation, Lys4 methylation, and Lys79 methylation on histone H3 [10,11] and tetraacetylation of Lys5, Lys8, Lys12 and Lys16 on histone H4 [12], however, identities of the "effector" proteins that may bind these marks remain elusive. Another mechanism of epigenetic gene regulation may also be encoded in the expression and exchange of histone gene family members (variants) [13,14], exemplified by the enrichment of the histone H2A family member, macroH2A on the X chromosome [15]. As appropriate regulation of gene-specific expression is critical to normal cell cycle progression and differentiation, and is disrupted in various disease states, interest continues to grow in the dynamics of histone modification and variant expression.

Interest in chromatin modification has grown particularly rapidly in the neurosciences. The mechanisms of action of a variety of neurological processes or disorders, and treatments for these disorders, may involve regulation of gene expression in various pathways which can be influenced by histone post-translational modifications. For example, it has been reported that an increase in histone H3 (but not H4) acetylation correlates with the induction of long term memory formation in the CA1 area of the hippocampus following contextual fear conditioning in mice [16]. This study furthermore determined that induction of long term memory potential was enhanced by the administration of the histone deacetylase inhibitors trichostatin A or sodium butyrate which elevate levels of histone acetylation. Changes in overall chromatin structure and histone modifications have also been described in the suprachiasmatic nucleus (SCN) when animals are exposed to light pulses aimed at resetting their circadian rhythm cycles [17]. Specifically, these discrete phase-resetting light pulses increase the acetylation of histone H3 and H4 associated with the promoter regions of Per1 and Per2 genes (important proteins involved in the transcriptional feedback loop of the circadian clock) and also increase overall histone H3 phosphorylation in the SCN. Finally, several reports have investigated and determined that histone post-translational modifications may be involved in regulation of events related to acute and chronic seizures, drug induced neuroadaptations, schizophrenia or bipolar disorders, and several different histone deacetylase compounds are currently being tested for antipsychotic effects [18–22].

Many investigations of histone PTMs have relied upon using site-specific antibodies to detect modifications. However, due to limitations affecting the use of these antibodies, including cross-reactivity and loss of specificity due to other modifications within the recognized epitope (epitope occlusion) [23], mass spectrometry has been increasingly used for the characterization of histone PTMs in both qualitative and quantitative manners [24–35]. Bottom Up mass spectrometric sequencing has been primarily used to analyze histone PTM states [25–29]. Although Bottom Up methods have advantages in sensitivity (largely due to the ionization of some peptides being better than intact protein), especially when coupling peptide analysis with on-line nanoLC–MS/MS techniques, Top Down mass spectrometry has some inherent properties that make it attractive for histone PTM investigations. Top Down analysis of proteins is somewhat simpler in nature, as the Bottom Up analysis of proteins involves detecting and interrogating many more precursor ions from a complex mixture of many peptides. More importantly, the assignment of PTM combinations is practically impossible with a Bottom Up approach unless the PTMs reside on the same peptide, so the discovery of a true comprehensive combinatorial histone code appears well-suited for Top Down mass spectrometry [30–35]. This most recently propelled by the major advancement of Electron Transfer Dissociation by the Hunt lab [35].

In this report, we detail the first analysis of histones from brain chromatin using electron capture dissociation (ECD) mass spectrometry from whole rat brain and selected brain sub-sections. Results categorized all the H2A and H2B gene family members that are expressed in the brain, as well as some low occupancy PTMs associated with these proteins. Interrogation of histones H4 and H3 by ECD allowed for the assignments of PTMs to several sites within each protein. Furthermore, we have adapted an ECD-based analysis of the largest core histone (H3) by targeting the first 1–50 residues as recently described by Hunt and co-workers [35]. Analysis of all four histones from whole brain and brain sub-sections including the cerebral cortex, cerebellum and hypothalamus indicate that no major differences in histone PTM profiles or variant expression exist between the tissues, except for one major finding: histone H3 Lys9 trimethylation is enriched in the cerebellum, the significance of which remains unknown. This work highlights the potential that Top and Middle Down mass spectrometry hold for histone protein characterization.

2. Experimental

2.1. Isolation and purification of core histones from rat brain tissue

Core histones were extracted from whole brain and other brain subsections including the cerebral cortex, cerebellum and hypothalamus from 7- to 8-week-old Sprague–Dawley rats of mixed gender (Pel-Freez Biologicals, Rogers, AR). Frozen brain tissue was slightly thawed and diced into small cubes and diluted with 10 volumes of nucleus isolation buffer (15 mM Tris–HCl; pH 7.5), 60 mM KCl, 11 mM $CaCl_2$, 5 mM NaCl, 5 mM $MgCl_2$,

250 mM sucrose, 1 mM dithiothreitol, 5 nM microcystin-LR, 500 μM 4-(2-aminoethyl) benzenesulfonyl fluoride (AEBSF) and 10 mM sodium butyrate, 0.3% NP-40) before homogenization using a PT 3000 Polytron Homogenizer (Littau, Switzerland). Nuclei were pelleted by centrifugation, washed with nucleus isolation buffer (not containing the 0.3% NP-40) and then histones were extracted with 0.4N H_2SO_4 before being recovered by trichloroacetic acid (TCA) precipitation. Purity of histone extractions was assessed by running an aliquot of the total histone extract on an 18% SDS-PAGE gel followed by Coomassie blue staining. Separation of total histones was achieved by loading about 100 μg of total histones onto a 4.6 mm × 250 mm C18 column (Vydac, Hesperia, CA) for reverse-phase high performance liquid chromatography (RP-HPLC) (System Gold, Beckman Coulter, Fullerton, CA). Histones were separated using a gradient of 30–60% solvent B in 100 min (solvent A = 5% acetonitrile (MeCN) in 0.2% trifluoroacetic acid (TFA) and solvent B = 90% MeCN in 0.188% TFA). All RP-HPLC fractions were dried to completion and resuspended in 25–50 μL of deionized water for mass spectrometry analysis.

2.2. Isolation of the amino-terminus of histone H3 (1–50 residues)

Additionally, purified histone H3 from pooled RP-HPLC fractions was digested by endoproteinase Glu-C (Sigma, St. Louis, MO) as previously described [35]. After dilution of the H3 sample originally dissolved in H_2O with 50 μL of 100 mM ammonium acetate buffer solution (pH 4), the sample was incubated with the protease at a substrate:enzyme ratio of 10:1 at room temperature for 4 h and the reaction was quenched by freezing. The 1–50 amino terminus of histone H3 produced by Glu-C digestion was then purified from the digestion mixture using RP-HPLC fractionation as described above. However, the gradient used to fractionate the digestion mixture was a 1% solvent B per minute gradient (solvent A = 5% acetonitrile, MeCN, in 0.2% trifluoroacetic acid, TFA, and solvent B = 90% MeCN in 0.188% TFA). The RP-HPLC fractions corresponding to the 1–50 residue fragment of histone H3 were dried to completion and resuspended in 20 μL of deionized water for mass spectrometry analysis.

2.3. Mass spectrometry analysis by electrospray ionization Fourier-transform mass spectrometry

Intact histones and the 1–50 histone H3 fragment were diluted with electrospray solution consisting of water and methanol (1:1) and 1% formic acid. All data were acquired on a home-built 8.5 Tesla quadrupole-FTMS in positive ion mode fitted with a NanoMate 100 (Advion BioSciences, Ithaca, NY) to produce the nanospray [36]. The NanoMate used ~12 μL of solution to automatically establish the spray. The capillary was heated by applying 4 A and the voltage was set at 2160 V. Various charge states of the histone proteins were selectively enhanced using the instrument's quadrupole and further filtered using Stored Waveform Inverse Fourier Transform (SWIFT) excitation [36]. For MS/MS experiments of selected ion species, electron capture dissociation (ECD) was utilized with a filament bias of approximately 9 V, using 25–200 loops of 8 ms electron pulses. Five amperes were applied to a dispensor cathode filament (Heatwave Technologies, Crescent Valley, BC) and ~10 V were applied on the grid potential. Data was collected using the modular ICR data acquisition system (MIDAS) [37]. Fragment ion data collected were analyzed using THRASH and/or manually interpreted. All M_r values of intact and fragment ions are reported for the neutral monoisotopic species.

3. Results and discussion

3.1. Analysis of histone H2B and H2A gene family members and PTMs

Acid-extracted total histones from whole rat brain tissue were fractionated on a C18 column by reversed-phase high performance liquid chromatography (RP-HPLC) as shown in Fig. 1A. Histone H2B is the first core histone to elute followed by a peak containing histone H2A gene family members. A peak containing histone H4 elutes next followed by another set of peaks containing more histone H2A proteins. Lastly, three peaks corresponding to the histone H3 variants H3.2, H3.3 and H3.1 elute several minutes later (Fig. 1A). Broadband spectrum of the intact H2B forms followed by quad-isolation (Fig. 1B and C) resulted in signal enhancement by approximately 15-fold. Characterization of H2A and H2B variants and their modifications was completed by SWIFT isolation of individual peaks followed by ECD (Fig. 1C and D). Three unmodified H2B variants are expressed in rat brain tissue: H2B 291B (M_r 13,766.5 Da, gi #34876384), H2B 291B (M_r 13,780.5 Da, gi #27693406) and H2Ba (M_r 13,854.5 Da, gi #27671691) (Table 1). ECD confirmed the existence of a mixture of H2B 291B (M_r 13,780.5 Da gi #27693406) and methylated H2B 291B (M_r 13,766.5 Da

Table 1
Histone H2A and H2B variants and post-translational modifications expressed in rat brain

Histone	NCBI gi #	Calc. mass (Da)[a]	Exp. mass (Da)[b]	PTMs
H2B 291B	34876384	13766.5	13767.2	None
H2B 291B	34876384	13780.5	13781.7	Monomethyl
H2B 291B	27693406	13780.5	13781.7	None
H2B 291B	34876384	13808.5	13808.9	Monoacetyl
H2B 291B	27693406	13808.5	13808.9	Dimethyl
H2B 291B	27693406	13822.5	13823.1	Trimethyl
H2Ba	27671691	13854.5	13855.1	None
H2A.1[c]	122009	13995.7	13996.8	N-Ac
H2A.F/Z	27697448	13369.4	13369.7	None
H2A.Z	55562729	13413.5	13413.6	None
H2A/1	34876391	14021.9	14022.1	N-Ac
H2A.1	27686415	14037.9	14038.1	N-Ac

[a] Calculated molecular weights of unmodified and modified sequences; all with loss of start methionine.
[b] All values are for the neutral, monoisotopic species.
[c] This form without any modifications has a M_r 13,937.8 Da, the calculated mass reported includes oxidation in addition to N-terminal acetylation (13,937.8 + 15.9 + 42.01 = 13,995.7 Da).

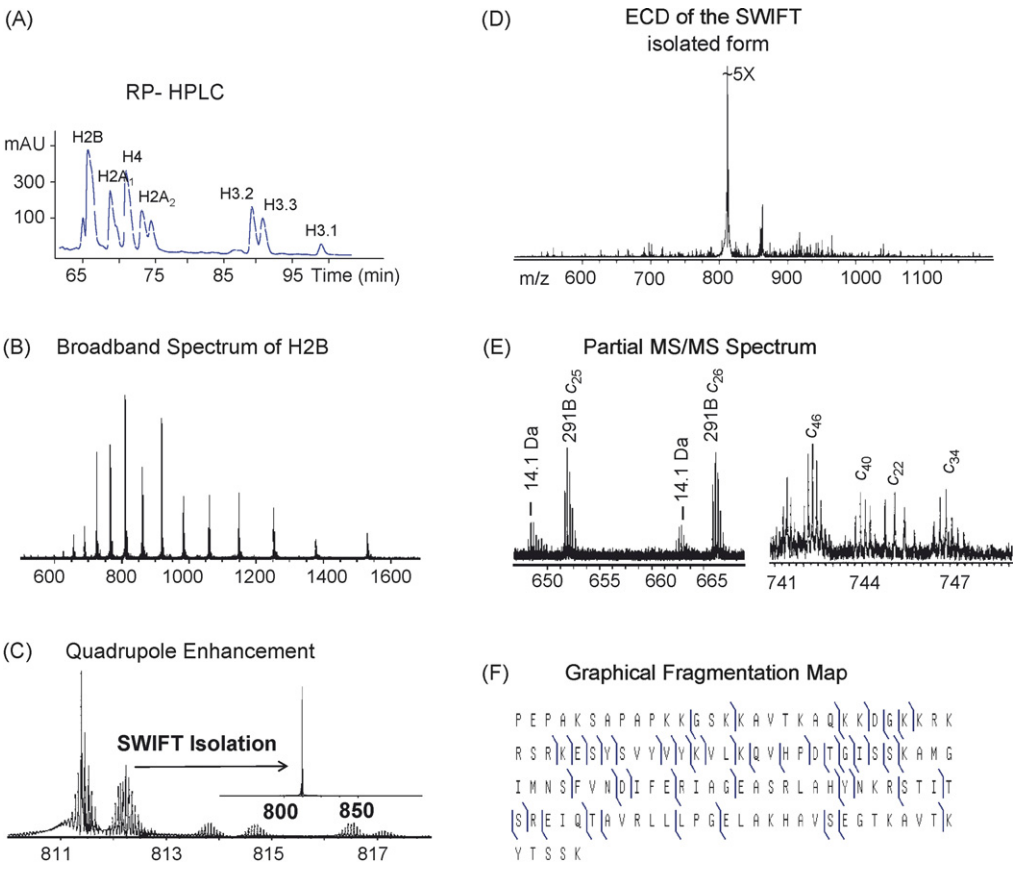

Fig. 1. Characterization of histone H2B form rat brain via Top Down mass spectrometry: (A) core histone peaks from a RPLC chromatogram, (B) broadband spectrum of intact histone H2B from rat brain tissue, (C) quadrupole enhancement of the 17+ charge state with SWIFT isolation, (D) MS/MS (ECD) of the quad- and SWIFT-isolated H2B form, (E) representative ECD fragment ions and (F) ProSight PTM fragmentation map with c and $z^{\bullet}$ ions indicated.

gi #34876384) for the peak with a M_r of 13,781.7 Da. Several *c*-type fragment ions from H2B 291B (M_r 13,780.5 Da, gi #27693406) have satellite peaks of −14.1 Da corresponding to H2B 291B gi #34876384 (Fig. 1E). H2B 291B (M_r 13,766.5 gi #34876384) and H2B 291B (M_r 13,780.5, gi #27693406) differ from each other by two amino acids. H2B 291B gi #27693406 has a D (aspartic acid) at position 2 (without counting the first methionine) and a V (valine) at position 21 (Fig. 1F). H2B 291B gi #34876384 has a E (glutamic acid) instead of a D (aspartic acid) at position 2 making it +14 Da heavier, however at position 21 this form has an A (alanine) instead of a V (V to A shift is −28 Da) making it −28 + 14 = −14 Da total less than H2B 291B gi #27693406. In order to be present on the 13,781.7 Da peak H2B 291B gi #34876384 has to be methylated. Histone H2B 291B gi #27693406 fragment ion c_{19} has a +14 Da satellite peak and c_{20} is +14 Da heavier. These fragment ions are evidence for the presence of H2B 291B gi #34876384. Up to residue 20, H2B 291B gi #34876384 is 14 Da heavier than H2B 291B gi #27693406 since the first form has an E (glutamic acid) at position 2 while the second form has a D (aspartic acid). Fragment ions c_{25}, c_{26}, c_{32}, c_{35}, c_{39}, c_{42} all have −14 Da satellite peaks. All these fragment ions are after residue 21 which is a V (valine) for H2B 291B gi #27693406 form and A (alanine) for gi #34876384 form. The −14 Da satellite peaks confirm the presence of H2B 291B gi #34876384 since after residue 21 their net mass is −14 Da (D to E = +14, V to A = −28) less than H2B 291B gi #27693406. The c_{42} is the last fragment ion with a −14.1 Da satellite peak; all the c fragment ions after this residue are an isobaric mixture of H2B 291B gi #27693406 and methylated H2B 291B gi #34876384 typified by c_{46} in Fig. 1E. All rat H2B forms have two methionines in their sequence with the first one of them at position 59. Partial oxidation of this residue would result in H2B 291B gi #34876384 (M_r 13,766.5 + 15.9 = 13,782.4 Da) to be potentially present in the observed isotopic distribution (M_r 13,781.7 Da). The first evidence for an isobaric mixture of oxidized H2B 291B gi #34876384 (M_r 13,766.5 Da) and H2B 291B gi #27693406 (M_r 13,780.5 Da) would be the absence of −14 Da satellite peaks for fragment ions after residue 59. ECD fragment ions are consistent with the last observed −14 Da satellite peak corresponding to c_{42}. This leads us to conclude that H2B 291B gi #34876384 (M_r 13,766.5 Da) is methylated at one of the two lysines from residue 43 to residue 46.

H2B 291B gi #27693406 (M_r 13,780.5 Da) was also found to be dimethylated at the same lysine or monomethylated at two different lysines simultaneously up to residue 26, while H2B 291B gi #34876384 (M_r 13,766.5 Da) was acetylated (−0.9 ppm) in one of the three total lysines from residue 13 to residue 17. The trimethylated form of H2B 291B gi #27693406 (M_r 13,780.5 Da) was also observed and as in the case of dimethylation, trimethylation was localized up to residue 26 (−12 ppm).

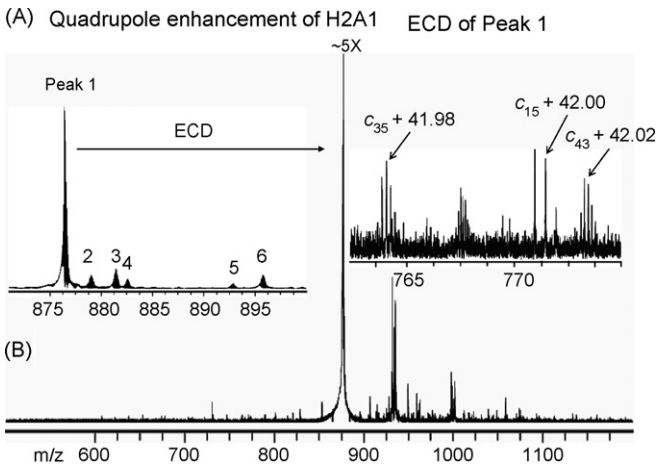

Fig. 2. Characterization of N-terminally acetylated histone H2A.1: (A) Quadrupole enhancement of histone H2A.1 (M_r 13,937.8 Da) and (B) ECD of Peak 1 (H2A.1) with fragment ions shifted by +42.0 Da corresponding to acetylation.

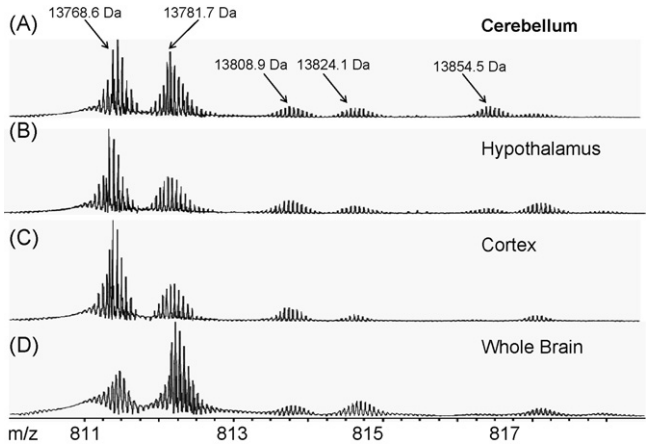

Fig. 3. Comparison of broadband spectra of histone H2B forms from (A) Cerebellum, (B) Hypothalamus, (C) Cortex and (D) Whole brain.

H2A variants from rat brain elute in two different RP-HPLC peaks that were separately characterized by MS/MS. Analysis of the first chromatographic peak revealed the presence of unmodified H2A.Z gi #55562729 (M_r 13,413.5 Da) and H2A.F/Z gi #27697448 (M_r 13,369.4 Da) (Fig. 2A, Peaks labeled 6 and 5, respectively and Table 1). ECD fragment ions (Fig. 2B) of the monoisotopic distribution labeled Peak 1 in Fig. 2A correspond to N-terminally acetylated H2A1 gi #122009 (M_r 13,937.8 Da). The mass discrepancy between acetylated H2A1 (13,937.8 Da + 42.01 Da = 13,979.8 Da) and the observed mass for peak 1 (M_r 13,996.8 Da) is due to oxidation. c_6 is the first ion reporting on N-terminal acetylation of H2A1 gi #122009 (M_r 13,937.8 Da). Acetylation of this variant at lysine 5 does not account for the shift of +42.02 Da observed from c_6 since there are no $z^\bullet$ ions that would include lysine 5 with a +42.02 Da mass shift.

H2A variants that eluted in the second chromatographic peak (H2A2) were also N-terminally acetylated. These variants include H2A/1 (M_r 14021.9 Da, gi #34876391) and H2A.1 (M_r 14,037.9 Da, gi #27686415) (Table 1). The profile of H2B expression from different brain subsections including cerebellum, cortex, and hypothalamus did not change (Fig. 3A–D). Similarly, the profile of H2A from rat brain subsections (cortex, hypothalamus and cerebellum) also did not show major differences from the profile of brain tissue (data not shown). Histones H2A and H2B from *Tetrahymena* and humans are not highly modified, however, they have more members of their gene families versus H3 and H4. In contrast to human histone H2B [34], histone variants expressed in rat brain tissue show evidence for a higher degree of PTMs, particularly methylation.

3.2. Characterization of histone H4 by Top Down mass spectrometry

ESI-FTMS analysis of the RP-HPLC peak that contained histone H4 (+15 charge state) from whole rat brain is shown in Fig. 4A. The broadband mass spectrum (Fig. 4A) revealed that the first detectable peak had a mass of 11,285.3 Da, which is 56 Da higher than predicted for the unmodified protein (11,229.3 Da) and is consistent with one acetyl group and a single methylation modification. As histone H4 from several organisms has been well characterized to contain an N-α-terminal acetylation (later confirmed by ECD), we suggest that this protein form is simply internally modified by the addition of one methyl group. The most abundant peak (11,299.5 Da) corresponded to the addition of an *N*-α-terminal acetylation mark and the addition of two methyl groups as this mass is 70 Da higher than predicted. The next most abundant peak contained a +112 Da mass shift in agreement with the addition of two acetyl groups (presumably one at the N-terminus), and two methyl groups (11,341.5 Da). A smaller peak that was assigned the addition of two acetyl modifications and a methyl modification was present at 11,327.5 Da. A very low level peak at 11,383.4 Da was also observed and this mass corresponds to the accumulation of three acetyl groups and two methyl marks (+154 Da shift). Additionally, two peaks (labeled with asterisks) were detected and ECD revealed that these were due to oxidation of Met85.

ECD fragmentation after quadrupole enhancement and SWIFT isolation of all H4 forms (+15 charge state) is shown in Fig. 4B. Fragment ion masses were calibrated using unmodified $z^\bullet$ ions (shown in zoom inset in Fig. 4B). ECD spectra confirmed that the N-terminus was acetylated, as a fragment ion at 417.2139 *m/z* was observed and is assigned as the c_4^+ ion with the addition of an acetyl group (calculated c_4^+ ion plus acetylation is 417.2106 Da, while the calculated c_4^+ ion with trimethylation is 412.2470 Da). Since the amino acids glycine, serine and arginine are not known to be modified by the addition of acetylation, and the N-terminus of H4 has been previously characterized by mass spectrometry as containing an acetyl group [23], we conclude that the N-terminus of histone H4 from rat brain is also *N*-α-acetylated. The next fragment ions that were indicative of modifications on histone H4 were detected spanning the 525–675 *m/z* region, shown as a zoomed inset in Fig. 4B. The set of c_{17}^{3+} fragment ions at 537.9838, and 551.9898 *m/z* were determined to come from the unmodified ion at the Lys16 residue and a +42 Da-shifted ion. Since sequence coverage of the protein

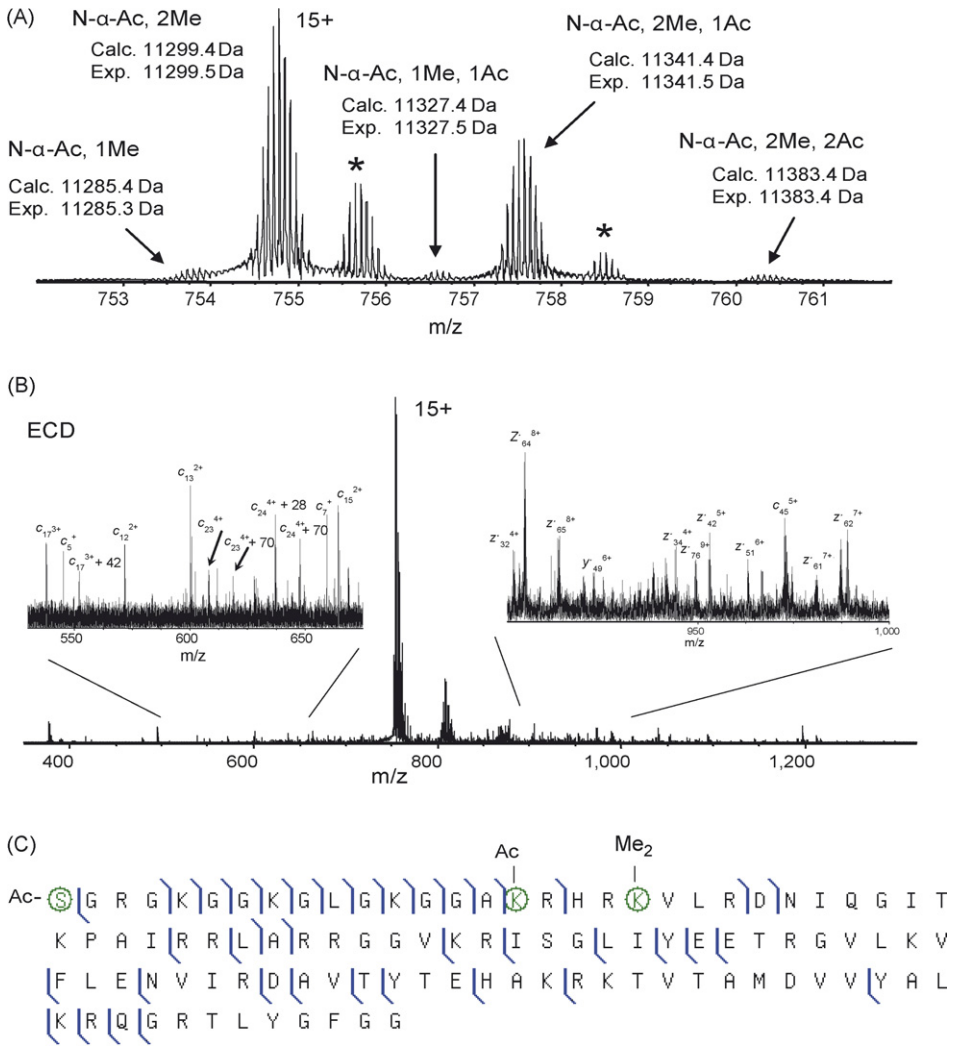

Fig. 4. Top Down characterization of histone H4 from whole rat brain: (A) Broadband mass spectrum of the 15+ charge state of histone H4. The monoisotopic mass is listed next to each species and oxidized species are indicated with an asterisk, (B) ECD mass spectrum of all precursor ions shown in (A) spanning the 753–763 *m/z* region, fragmented after quadrupole filter enhancement of the 15+ charge state and SWIFT isolation (∼200 scans). Zoom inset shows fragment ions corresponding to Lys16 and Lys20 post-translational modifications, as well as unmodified ions and (C) ECD fragment map generated from assigning the fragment ions shown in (B).

showed that Lys5, Lys8 and Lys12 were largely unmodified (see ECD fragment map Fig. 4C), the +42 Da shift was attributed to an acetylation modification on Lys16 (+1.63 ppm). A look at the c_{23}^{4+} and c_{24}^{4+} ions also revealed that mass shifts of +28 and +70 Da were present from the predicted unmodified ions. A 28 Da shift is consistent with a dimethylation at Lys20, which is another well-characterized mark on histone H4. The ion species at +70 Da (647.3877 *m/z*) is thus consistent with the addition of the dimethyl group on Lys20 plus the addition of one acetyl group at Lys16 (+3.55 ppm). It should be worth noting that the ion abundance ratios of the c_{24}^{4+} and c_{24}^{4+} +42 Da ions mirror the ratios of the intact protein ions (Fig. 4A). A weak signal corresponding to a second acetylation site at Lys12 was occasionally observed, but no other modifications on histone H4 were observed by our methods. We also examined histone H4 from specific brain sub-sections including the cerebral cortex, cerebellum and hypothalamus, and found no significant changes in the H4 PTM profiles (data not shown).

3.3. Middle Down mass spectrometry for enhanced analysis of histone H3 modifications

Histone H3 gene family members from whole rat brain tissue (and rat brain sub-sections cerebral cortex, cerebellum and hypothalamus) elute in three distinct reproducible peaks as labeled in Fig. 1A. H3.2 eluted first and was most abundant. With histone H3.2 sequences highly conserved across several different eukaryotic species such as in all mammals, *Xenopus* and *Drosophila* [38], it was targeted for ECD (Fig. 5). Fig. 5A shows the broadband mass spectrum obtained for the 18+ charge state of histone H3.2. The theoretical mass of H3.2 is 15,247.5 Da and is very close to the experimental mass of the first peak observed in broadband mass spectrum (15,247.7 Da). As can be seen, several peaks corresponding to the addition of one methyl equivalent mass can be detected in the spectrum, with the apex peak containing 10 methyl equivalents. Top Down mass spectrometry characterization of the modification sites of H3.2

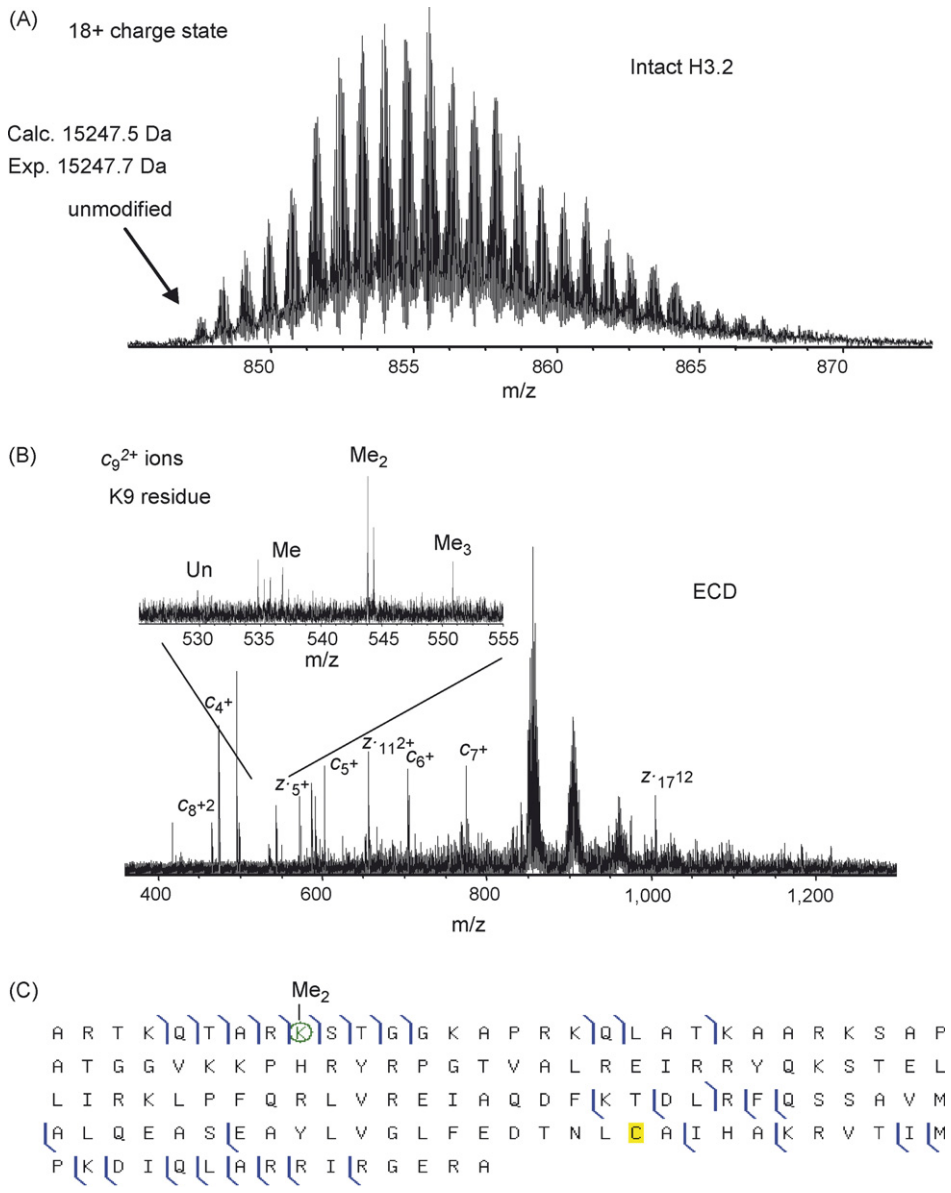

Fig. 5. Top Down mass spectrometry analysis of intact histone H3.2 from whole rat brain: (A) broadband mass spectrum of the 18+ charge state of H3.2. The first detectable peak was observed to have a mass in agreement with the unmodified form, (B) ECD mass spectrum (∼300 scans summed) of the precursor ions isolated (all modified forms, 845–870 *m/z* range) in (A) following quadrupole enhancement and SWIFT isolation. Zoom inset shows c_9^{2+} ions corresponding to modifications at Lys9 and (C) ECD fragment map generated from histone H3.2 after assigning the fragment ions shown in (B).

utilized ECD fragmentation of all modified forms *en masse* as previously shown [32], following quadrupole enhancement of all 18+ species and subsequent SWIFT isolation. A typical ECD mass spectrum of H3.2 is shown in Fig. 5B, and the zoom inset of the region spanning the 528–555 *m/z* range shows a set of c_9^{2+} ions corresponding to Lys9 of H3, a residue which is well-documented to contain both methylation and acetylation by both biological and mass spectrometry based methods [4,24]. The c_9^{2+} ions corresponding to unmodified and monomethylated Lys9 modifications (529.8355 and 536.8408 *m/z*, respectively) were in low abundance, while the most abundant modification at Lys9 was found to be the dimethylated ion at 543.8449 *m/z*. A peak corresponding to either trimethylation or acetylation ($\Delta m = 0.036$ Da) was observed at 550.8547 *m/z*. Accurate mass of the c_9^{2+} ion confirmed the modification as trimethylation (+0.7 ppm error) and not acetylation.

Nonetheless, some of the more highly abundant ions in the ECD spectrum were assigned to unmodified $z^{\bullet}$ ions, as depicted in the ECD fragment map generated for histone H3.2 (Fig. 5C). This is somewhat unfortunate as the vast majority of histone H3 modifications are known to be found at the N-terminal region of the protein [4,6]. Therefore, the observed $z^{\bullet}$ ions do not significantly contribute to mapping the lysine modifications [32]. To improve PTM localization, histone H3 variants were digested with endoproteinase Glu-C to release a polypeptide spanning residues 1–50 (containing nearly all previously known modified residues), which can be easily generated and isolated using RP-HPLC as recently demonstrated by Hunt and co-workers

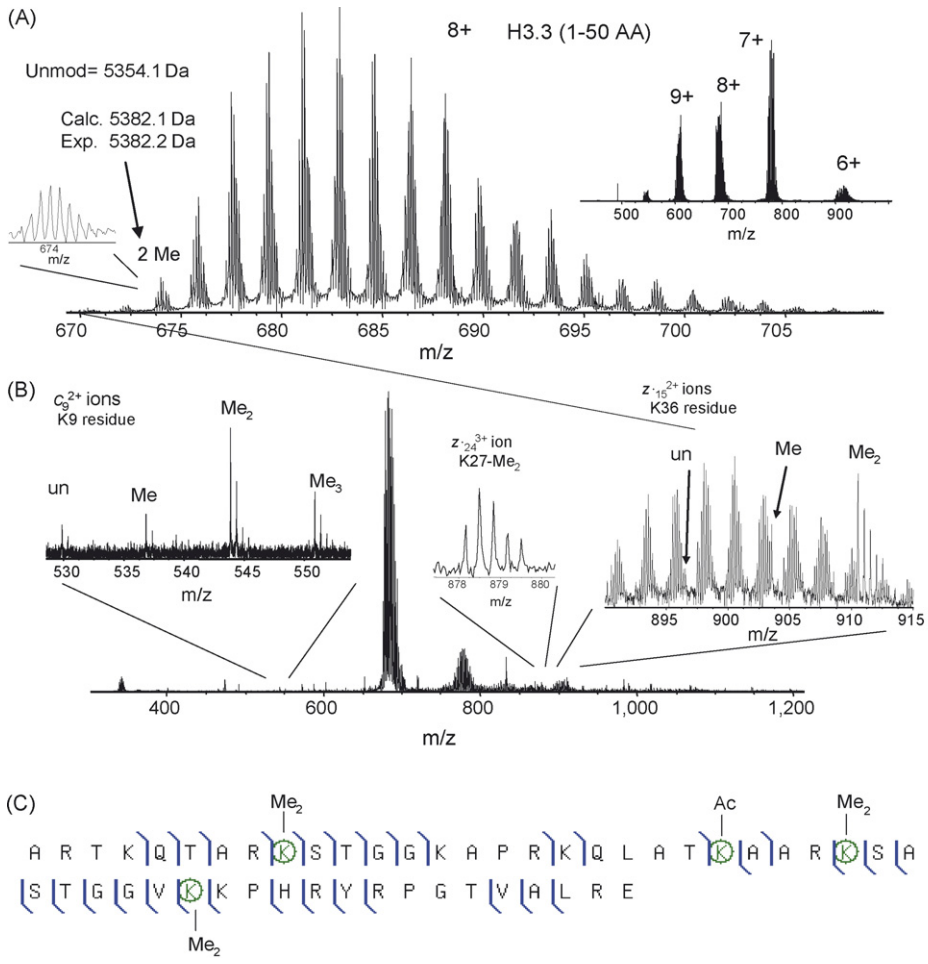

Fig. 6. Middle Down ECD mass spectrometry analysis of whole rat brain histone H3.3 after GluC digestion and RP-HPLC isolation of the 1–50 residue fragment: (A) broadband mass spectrum of the 8+ charge state of the 1–50 fragment from histone H3.3. Inset mass spectrum shows the distribution of charge states from the H3.3 1–50 residue fragment, (B) ECD mass spectrum of the precursor ions isolated (all modified forms, 670–710 *m/z* range) in (A) following quadrupole enhancement and SWIFT isolation (∼300 scans). Zoom insets show ions corresponding to Lys9, Lys36 and Lys27 post-translational modifications and (C) ECD fragment map of histone H3.3 (1–50 residue fragment) generated from ECD spectrum shown in (B).

[35,39]. The analysis of the 1–50 fragment of histone H3 is herein referred to as Middle Down mass spectrometry, as we strategically digested H3 to produce a few large peptides, rather than the multitude of smaller peptides commonly created in trypsin-mediated Bottom Up approaches. It is worthy to note that this concept has been previously reported for other proteins by Fenselau and co-workers [40,41]. Fig. 6A shows the broadband mass spectrum of the 8+ charged histone H3.3 1–50 species centered around 685 *m/z* and demonstrates the usefulness of the smaller 1–50 piece to baseline resolve. In the gas phase, the 1–50 residue fragment exists substantially as 6+, 7+, 8+ and 9+ charged species as shown in the upper right hand inset in Fig. 6A. The first peak of the 8+ charged species was found to have a mass of 5382.2 Da compared to the calculated mass of the unmodified H3.3 1–50 fragment of 5354.1 Da. The mass difference between these two was approximately 28 Da, indicating that the first peak contained two methylations. A similar distribution of masses separated by ∼14 Da was detected as in the broadband mass spectrum of intact H3.3, with the apex of the peaks for the 1–50 fragment containing about 7 methyl equivalent groups as opposed to about 10 methyl equivalents for the intact H3.3 protein. Indeed, a tryptic digestion Bottom Up peptide analysis of rat brain histone H3.3 revealed that modifications to the C-terminal portion of the protein did exist at Lys79 (mono and dimethylation, data not shown). Additionally, we noted that a larger number of phosphate adducts were present on the intact H3 versus the 1–50 fragment, and these adducts being a multiple of 14 Da (phosphate = 98 Da) could also add complexity to the H3 peak distribution. This may also explain why a lower apex of methyl equivalent groups was observed on the H3 1–50 fragments as opposed to intact protein. We decided to continue to analyze the 1–50 H3 fragment by ECD as the N-terminus of H3 is highly modified and significant as it protrudes from the nucleosome recruiting effector proteins such as HP1 [8,42].

An ECD mass spectrum of the H3.3 1–50 residue polypeptide is displayed in Fig. 6B. As can be seen, a cleaner MS/MS spectrum (lower chemical noise level compared to Top Down data) was obtained after summing approximately the same number of scans (∼300). Ions reporting on Lys9 (c_9^{2+} ions) are shown in the upper left hand inset spanning the 528–555 *m/z*

region, and a similar methylation profile (un, mono, di and trimethyl (550.8562 Da, +3.5 ppm error)) was detected on the 1–50 fragment, as dimethylation of Lys9 was the most abundant modification. Significantly, we found that the $z^{\bullet}$ ions from the 1–50 fragment are very useful for assigning modifications to Lys36 ($z^{\bullet 2+}_{15}$ ion) and Lys27 ($z^{\bullet 3+}_{24}$ or $z^{\bullet 3+}_{27}$ ion), as shown in the inset zoom MS regions of Fig. 6B. An inset spanning the 895–915 *m/z* region shows the $z^{\bullet 2+}_{14}$ ions corresponding to Lys36 unmodified (896.5183 *m/z*), monomethylated (903.5270 *m/z*) and dimethylated (910.5291 *m/z*). No trimethylation or acetylation of Lys36 was recorded. Building on the profile of Lys36, ions corresponding to Lys27 ($z^{\bullet 3+}_{24}$) spanning the 859–883 *m/z* region were detected. A $z^{\bullet 3+}_{24}$ ion at 868.8231 *m/z* which is 28 Da higher than expected for the unmodified Lys27 residue $z^{\bullet}_{24}$ ion was seen and attributed to the abundant Lys36 dimethylation modification first indicated by the $z^{\bullet}_{15}$ ions and no or little modification at Lys27. However, $z^{\bullet 3+}_{24}$ ions at 873.5001, 878.1697 and 882.8435 *m/z*, respectively, demonstrate that besides Lys36 dimethylation, mono, di and trimethylation (+2.7 ppm), but not acetylation are observed at Lys27. The ion corresponding to Lys36 dimethylation and a possible dimethylation at Lys27 (4 methyl group equivalents above the unmodified $z^{\bullet 3+}_{24}$ ion) is shown as a zoom inset in Fig. 6B. Lys4 was found to be unmodified and monomethylated to a much lesser extent (c^{+}_{4} ions at 474.3162 *m/z* and 14 Da shifted at 488.3275 *m/z*, Fig. 6A). Reporter ions at Lys14 (c^{3+}_{17}) and Lys18 (c^{3+}_{18}) indicated that an overwhelming level of unmodified residues occupy those sites. The c^{3+}_{24} ions reporting on the Lys23 residue showed that the most abundant ion was at 861.1871 *m/z* which is +28 Da higher than expected for an unmodified residue ion (calculated unmodified c^{3+}_{24} ion = 851.8444 *m/z*). This +28 Da shift is attributed largely to the abundant dimethylation at Lys9 rather than modifications at K14, K18 or K23. However, a weaker ion signal at 875.1957 *m/z* corresponding to a dimethylation (presumably at Lys9) and an acetylation (+4.8 ppm) indicate that K23 is an acetylation site on H3.3 from rat brain tissue. A typical ECD fragment map of the H3.3 1–50 residue fragment showing some of the more abundant modifications is shown in Fig. 6C, and more importantly displays the improved sequence coverage for the amino-terminal polypeptide over the intact H3 protein. The same modification sites were noted on the histone H3.2 variant after Middle Down analysis using ECD. These analyses are consistent with H3 modifications characterized by mass spectrometry from mouse cells [29].

Recent reports have detailed that H3 variants may be enriched in certain modifications. For example, in *Drosophila*, Henikoff and co-workers noted an enrichment of modifications associated with transcriptional activation, such as Lys4 methylation

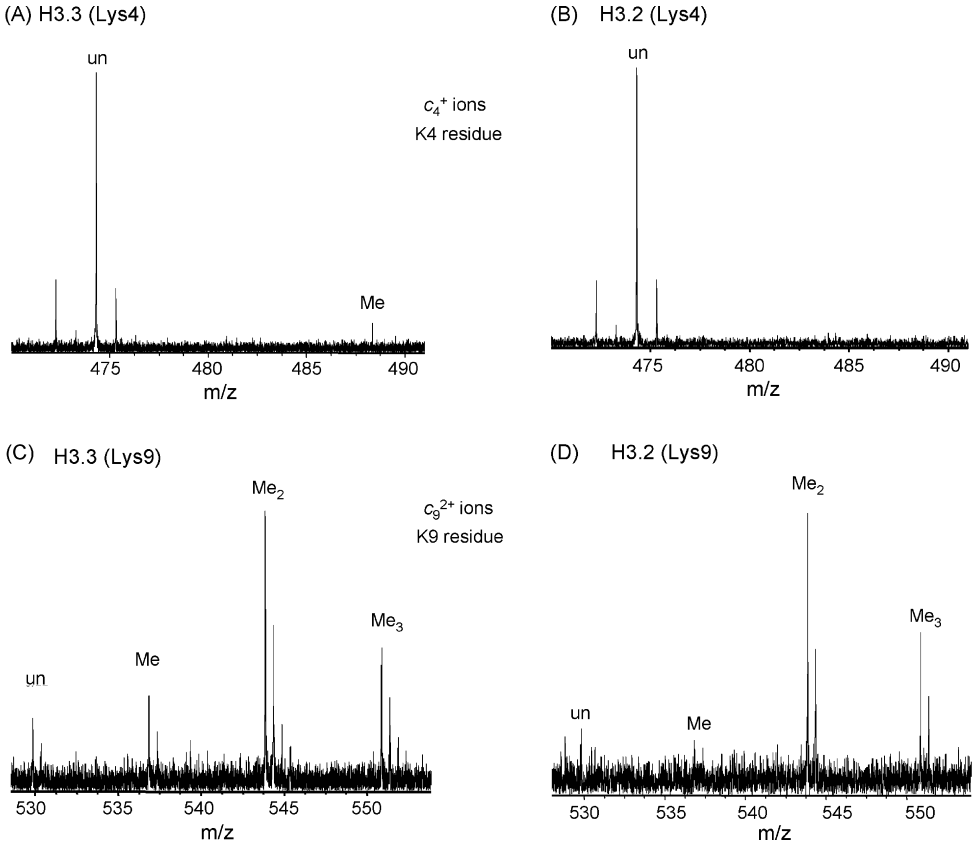

Fig. 7. Comparison of post-translational modifications on Lys4 (c^{+}_{4}) and Lys9 (c^{2+}_{9} ions) from histones H3.2 and H3.3 extracted from whole rat brain: (A) the c^{+}_{4} ions reporting on the modification states of Lys4 from histone H3.3. Monomethylation at a low level can be observed as the only modification at this site, (B) the c^{+}_{4} ions reporting on the modification states of Lys4 from histone H3.2. No modifications can be easily observed, (C) the c^{2+}_{9} ions reporting on the modification states of Lys9 from histone H3.3. The Lys9 residue was observed to exist in unmodified, monomethylated, dimethylated and trimethylated forms and (D) the c^{2+}_{9} ions reporting on the modification states of Lys9 from histone H3.2. A similar profile can be observed as in the H3.3 variant.

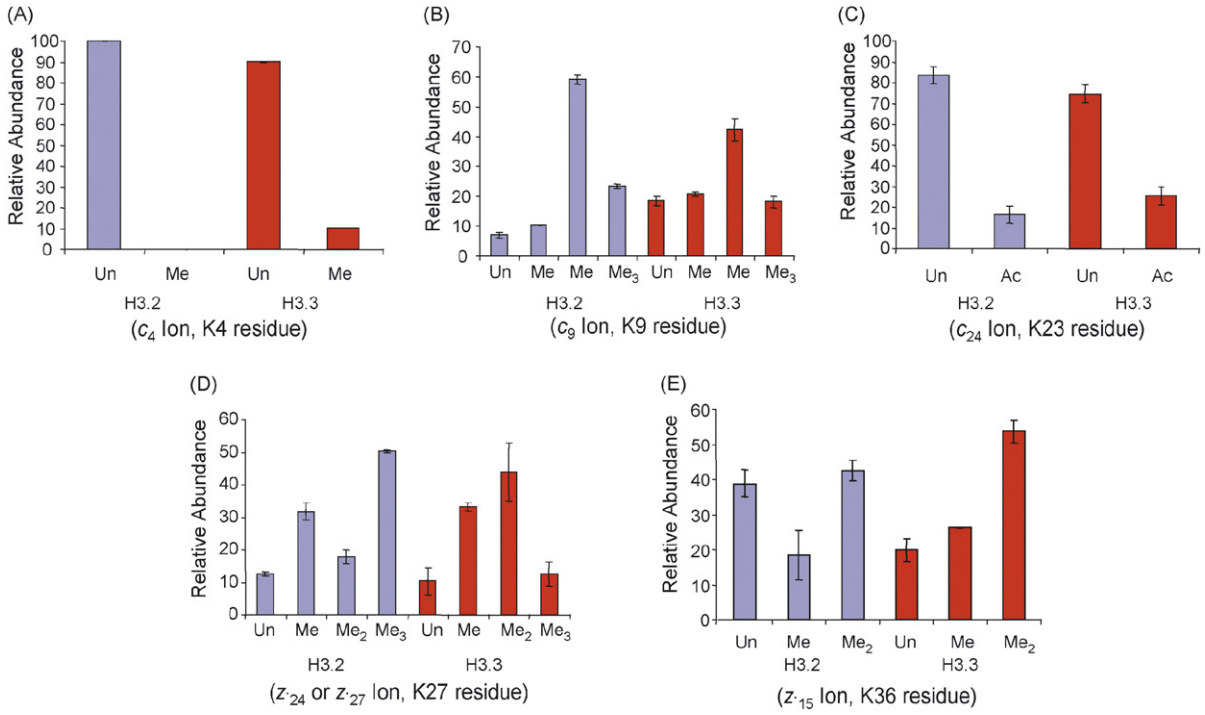

Fig. 8. Comparison of modifications observed in ECD generated c and z• ions from histones H3.2 and H3.3 (1–50 residue fragment) extracted from whole rat brain showing modifications at (A) Lys4, (B) Lys9, (C) Lys23, (D) Lys27 and (E) Lys36. The fractional occupancy was calculated from ECD of the +8 charged species. Histograms depict the average of three values and standard deviations are shown as error bars.

and acetylation of Lys14, Lys18 and Lys23 in H3.3 as compared to canonical H3 (H3.2 in mammals) [43]. These authors also found a decreased amount of Lys9 dimethylation (silencing mark) on H3.3 as well. Hake et al. also discovered a similar trend on human histone H3 variants extracted from HEK 293 cells as well [44]. Therefore, we decided to compare the modification profiles of the histone H3.2 and H3.3 variants to one another to see if any modifications were found to be enriched on either protein. Broadband profiles of the 1–50 fragments of each H3 variant displayed similar methyl equivalent distributions (data not shown). However, since certain lysine modifications are considered activation marks (Lys4 methylation, Lys36 methylation or acetylation at any lysine residue) and other lysine residues when modified are associated with gene silencing (Lys9 or Lys27 methylation) and broadband MS data cannot be used to determine modification sites, ECD data must be acquired to localize the PTM sites. Fig. 7 shows a side by side comparison of the c_4^+ ions reporting on the modified state of Lys4 and c_9^{2+} ions reporting on the modified state of Lys9 from rat brain histone H3.2 and H3.3 1–50 polypeptides. Fig. 7A and B display the c_4^+ ions and a marked increase in Lys4 monomethylation was observed on the H3.3 variant. Inspection of the c_9^{2+} ions from H3.3 and H3.2 (Fig. 7C and D, respectively) show that similar profiles are present on both variants at Lys9, but that small increases in unmodified and monomethylated species and a slight decrease in Lys9 dimethylation on the H3.3 variant were evident. Relative quantification of ion abundance ratios involved summing the first two isotopic peaks for each mass from the 8+ charged species, resulting in fragment ion relative ratios and these values were then converted to percent occupancy by dividing the indi-

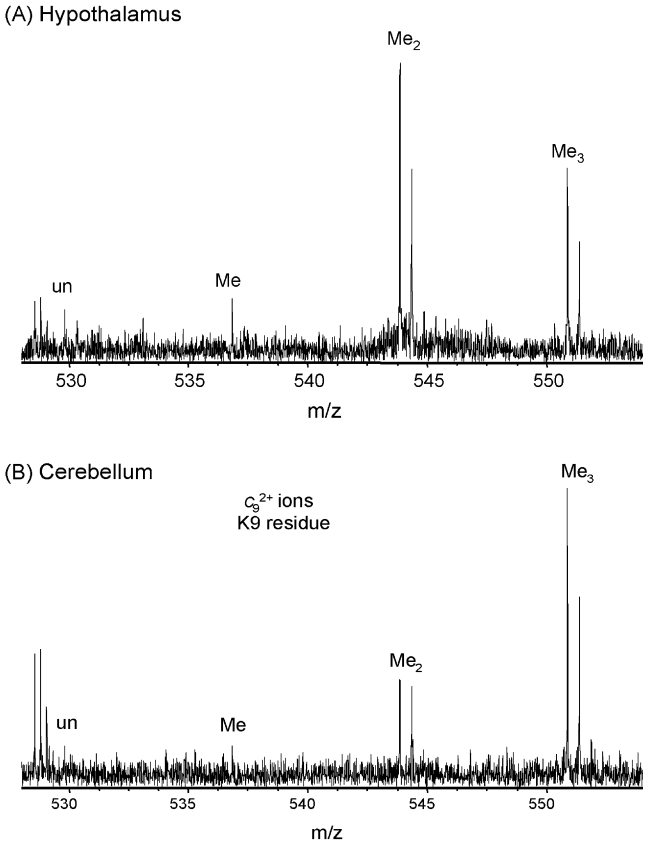

Fig. 9. Comparison of post-translational modifications on Lys9 (c_9^{2+} ions) from histone H3.2 (1–50 residues fragment) extracted from (A) hypothalamus and (B) cerebellum tissue.

vidual ion abundances by the total sum of the ion set as recently described [32]. The results of this quantification are summarized in bar graphs shown in Fig. 8A–E, reporting on the modification states of Lys4, Lys9, Lys23, Lys27 and Lys36, respectively. As can be seen in Fig. 8A, a slightly higher amount of Lys4 monomethylation can be detected on H3.3 compared to none detected on H3.2. Similar profiles of Lys9 modifications exist between the H3.2 and H3.3 variants, with a small but noticeable reduction of dimethylation and small increase in unmodified and monomethylated forms found for the H3.3 variant (Fig. 8B). No significant changes were observed at Lys23 between the H3 variants (Fig. 8C). Fig. 8D shows a shift in the most abundant Lys27 modification state between the H3 variants, as H3.2 has a slight enrichment in Lys27 trimethylation, while H3.3 contains more Lys27 dimethylation. Fig. 8E shows that the histone variant H3.2 contains a similar distribution of Lys36 dimethylation as H3.3 with slight differences in monomethylation and unmodified Lys36 levels. Our results from the comparison of the histone variants H3.2 and H3.3, while not as drastically impressive as those mentioned earlier from other eukaryotes [43] still exhibit a similar trend with H3.3 being slightly enriched with an activating mark (Lys4 methylation), and H3.2 being enriched with silencing marks (Lys27 trimethylation and more heavily methylated Lys9 forms).

Lastly, we also analyzed histone H3.2 and H3.3 from various brain sub-sections (cerebral cortex, cerebellum and hypothalamus) and compared the modification states of the H3 proteins to one another and also to the whole rat brain H3s. Our results show that no major differences can be detected at Lys4, Lys23, Lys27 or Lys36 from any of the aforementioned brain sub-sections. This is similar to the other histones as no large differences in the variant expression of H2A or H2B family members or H4 PTMs were seen in the different brain tissues. However, one major difference was noted in the distribution of K9 modifications from the cerebellum when compared to either whole brain, cerebral cortex or the hypothalamus tissue. Fig. 9 shows the modification states of the Lys9 residue (c_9^{2+} ions) from the H3.2 1–50 peptide from the hypothalamus (Fig. 9A) and cerebellum (Fig. 9B). The c_9^{2+} ions from the hypothalamus tissue have a similar distribution as whole brain (Fig. 9) and the cerebral cortex (data not shown) with the most abundant modification present being dimethylation of Lys9 followed by a lesser amount of Lys9 trimethylation and minute amounts of unmodified and monomethylated ions. However, in the cerebellum we discovered that the modification state of Lys9 is shifted to a higher degree of modification as the +42 Da species was the most abundant followed by the dimethylated species and very little amount of unmodified or monomethylated species present. The c_9^{2+} ion shifted by 42 Da from the unmodified ion was observed at 550.8532 *m/z*, which is consistent with trimethylation (−2.0 ppm error) versus an acetylation modification (+31 ppm error). This unexpected result may simply reflect

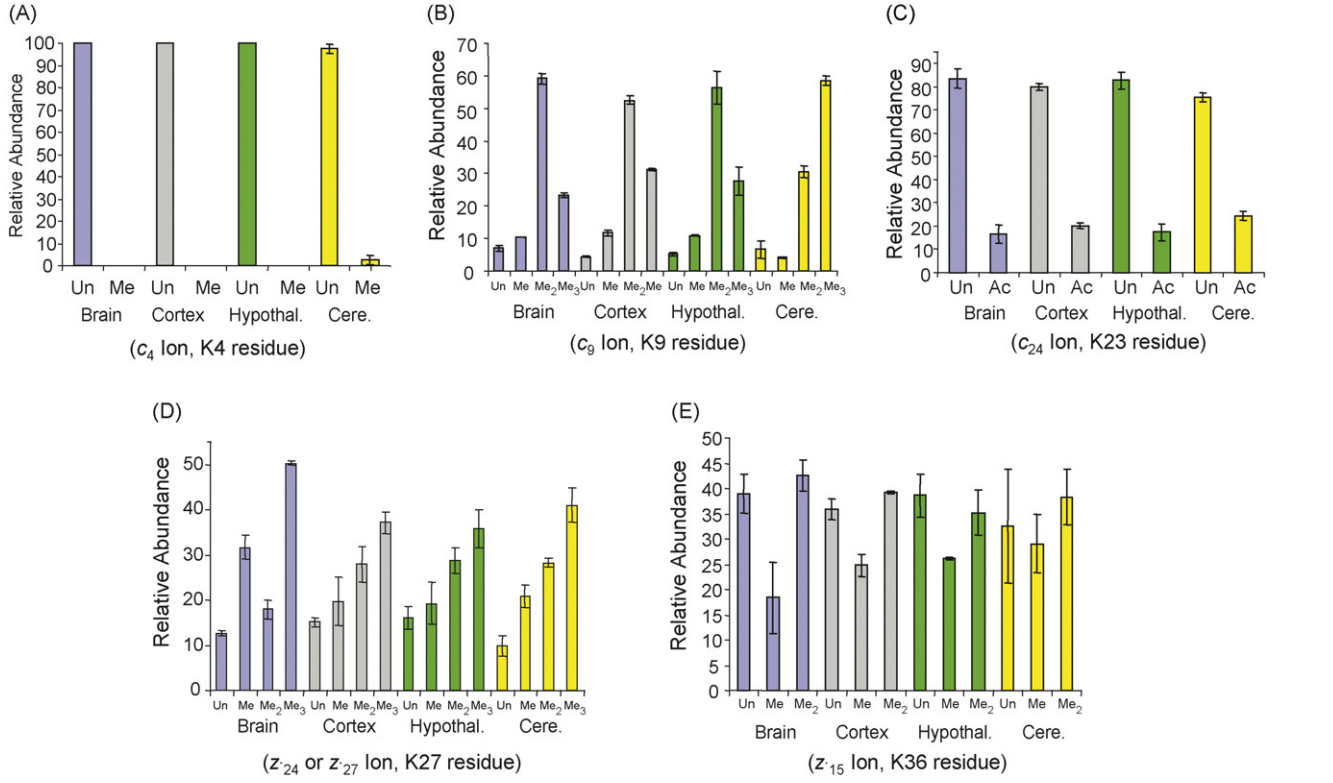

Fig. 10. Comparison of modifications observed in ECD generated c and z• ions from histone H3.2 (1–50 residue fragment) extracted from whole rat brain (Brain, blue), cerebral cortex (Cortex, grey), hypothalamus (Hypothal., green) and cerebellum (Cere., yellow) showing modifications at (A) Lys4, (B) Lys9, (C) Lys23, (D) Lys27 and (E) Lys36. The fractional occupancy was calculated from ECD of the +8 charged species. Histograms depict the average of three values and standard deviations are shown as error bars.

differences in the ratios of neurons to glia in the cerebellum compared to other brain regions, but it is intriguing to speculate that this enrichment of Lys9 trimethylation mediates higher degrees of transcriptional silencing through increased binding of HP1 that are significant with respect to cerebellum function. A complete look at all the modification states of Lys4, Lys9, Lys23, Lys27 and Lys36 are displayed in Fig. 10A–E for the histone H3.2 1–50 fragment. Consistent levels of all other modifications between all brain sub-sections were detected with the exception of the aforementioned Lys9 trimethylation increase in the cerebellum tissue. A similar enrichment of Lys9 trimethylation was also observed on histone H3.3 from cerebellum tissue as compared to the other brain tissues (data not shown).

4. Conclusion

Our work has shown the usefulness of using electron capture dissociation mass spectrometry for assessing histone post-translational modifications on all four core histones from brain chromatin. To our knowledge, these investigations are the first mass spectrometry analyses reported for histones from brain of any species. Top Down mass spectrometry analysis was used to probe the expression of specific histone H2A and H2B gene family members, and we found that the expression of these members does not vary significantly between different brain regions. Additionally, modest levels of post-translational modification were observed for H2A and H2B. Investigation of histone H4 revealed that the pattern of post-translational modifications did not differ significantly between the various brain regions. A Middle Down approach was utilized for improved analysis of H3 by ECD mass spectrometry. This method consisted of digesting the intact H3 using endoproteinase GluC and isolating the 1–50 fragment before interrogation by ECD fragmentation. Although the H3 post-translational modification profiles were similar between the different brain sub-sections, we discovered one large difference in that the level of H3 Lys9 trimethylation was higher in the cerebellum sample than in any of the other brain tissues. This research displays the feasibility and utility of electron capture dissociation mass spectrometry techniques for the identification of histone variants and post-translational modifications to afford a more precise view of the role of a histone code during key physiological processes.

Acknowledgements

The authors thank the National Institute of Health (N.L.K., GM #067193), the Packard Foundation, the Alfred P. Sloan Foundation, and a 2004 Camille Dreyfus Teacher-Scholar Award from the Dreyfus Foundation. The laboratory of C.A.M supported by the University of Illinois and the Roy J. Carver Charitable Trust (04-76). This work is also supported by the University of Illinois and the UIUC Neuroproteomics Center on Cell–Cell Signaling funded through PHS 1 P30 DA 018310. B.A.G. is supported by a post-doctoral fellowship from the Institute for Genomic Biology at the University of Illinois. D.F. Hunt is also acknowledged for his strong support of B.A.G., C.A.M. and N.L.K.

References

[1] K. Luger, A.W. Mader, R.K. Richmond, D.F. Sargent, T.J. Richmond, Nature 389 (1997) 251.
[2] G. Felsenfeld, M. Groudine, Nature 421 (2003) 448.
[3] C.A. Mizzen, C.D. Allis, Cell. Mol. Life Sci. 54 (1998) 6.
[4] B.D. Strahl, C.D. Allis, Nature 403 (2000) 41.
[5] M. Iizuka, M.M. Smith, Curr. Opin. Genet. Dev. 13 (2003) 154.
[6] T. Jenuwein, C.D. Allis, Science 293 (2001) 1074.
[7] B.M. Turner, Cell 111 (2002) 285.
[8] M. Lachner, D. O'Carroll, S. Rea, K. Mechtler, T. Jenuwein, Nature 410 (2001) 116.
[9] J.A. Daniel, M.G. Pray-Grant, P.A. Grant, Cell Cycle 4 (2005) 919.
[10] B.E. Bernstein, E.L. Humphrey, R.L. Erlich, R. Schneider, P. Bouman, J.S. Liu, T. Kouzarides, S.L. Schreiber, Proc. Natl. Acad. Sci. USA 99 (2002) 8695.
[11] H.H. Ng, D.N. Ciccone, K.B. Morshead, M.A. Oettinger, K. Struhl, Proc. Natl. Acad. Sci. USA 100 (2003) 1820.
[12] C.A. Johnson, L.P. O'Neill, A. Mitchell, B.M. Turner, Nucl. Acids Res. 26 (1998) 994.
[13] T. Kusch, L. Florens, W.H. Macdonald, S.K. Swanson, R.L. Glaser, J.R. Yates, S.M. Abmayr, M.P. Washburn, J.L. Workman, Science 306 (2004) 2084.
[14] K. Sarma, D. Reinberg, Nat. Rev. Mol. Cell Biol. 6 (2005) 139.
[15] C. Costanzi, J.R. Pehrson, Nature 393 (1998) 599.
[16] J.M. Levenson, K.J. O'Riordan, K.D. Brown, M.A. Trinh, D.L. Molfese, J.D. Sweatt, J. Biol. Chem. 279 (2004) 40545.
[17] Y. Naruse, K. Oh-hashi, N. Iijima, M. Naruse, H. Yoshioka, M. Tanaka, Mol. Cell Biol. 24 (2004) 6278.
[18] Y. Huang, J.J. Doherty, R. Dingledine, J. Neurosci. 22 (2002) 8422.
[19] C.M. Colvis, J.D. Pollock, R.H. Goodman, S. Impey, J. Dunn, G. Mandel, F.A. Champagne, M. Mayford, E. Korzus, A. Kumar, W. Renthal, D.E. Theobald, E.J. Nestler, J. Neurosci. 25 (2005) 10379.
[20] R. Sharma, Schizophr. Res. 72 (2005) 79.
[21] M.V. Simonini, L.M. Camargo, E. Dong, E. Maloku, M. Veldic, E. Costa, A. Guidotti, Proc. Natl. Acad. Sci. USA 103 (2006) 1587.
[22] J.M. Levenson, J.D. Sweatt, Nat. Rev. Neurosci. 6 (2005) 108.
[23] P. Cheung, Methods Enzymol. 376 (2004) 221.
[24] S.C. Galasinski, D.F. Louie, K.K. Gloor, K.A. Resing, N.G. Ahn, J. Biol. Chem. 277 (2002) 2579.
[25] K. Zhang, H. Tang, L. Huang, J.W. Blankenship, P.R. Jones, F. Xiang, P.M. Yau, A.L. Burlingame, Anal. Biochem. 306 (2002) 259.
[26] F. Chu, D.A. Nusinow, R.J. Chalkley, K. Plath, B. Panning, A.L. Burlingame, Mol. Cell. Proteomics 5 (2006) 194.
[27] M.A. Freitas, A.R. Sklenar, M.R. Parthun, J. Cell Biochem. 92 (2004) 691.
[28] B.A. Garcia, S.A. Busby, C.M. Barber, J. Shabanowitz, C.D. Allis, D.F. Hunt, J. Proteome Res. 3 (2004) 1219.
[29] R.R. Cocklin, M. Wang, J. Protein Chem. 22 (2003) 327.
[30] J.J. Pesavento, Y.B. Kim, G.K. Taylor, N.L. Kelleher, J. Am. Chem. Soc. 126 (2004) 3386.
[31] K.F. Medzihradszky, X. Zhang, R.J. Chalkley, S. Guan, M.A. McFarland, M.J. Chalmers, A.G. Marshall, R.L. Diaz, C.D. Allis, A.L. Burlingame, Mol. Cell. Proteomics 3 (2004) 872.
[32] C.E. Thomas, N.L. Kelleher, C.A. Mizzen, J. Proteome Res. 5 (2006) 240.
[33] M.T. Boyne, J.J. Pesavento, C.A. Mizzen, N.L. Kelleher, J. Proteome Res. 5 (2006) 248.
[34] N. Siuti, M.J. Roth, C.A. Mizzen, N.L. Kelleher, J.J. Pesavento, J. Proteome Res. 5 (2006) 233.
[35] J.J. Coon, B. Ueberheide, J.E. Syka, D.D. Dryhurst, J. Ausio, J. Shabanowitz, D.F. Hunt, Proc Natl. Acad. Sci. USA 102 (2005) 9463.
[36] S.M. Patrie, J.P. Charlebois, D. Whipple, N.L. Kelleher, C.L. Hendrickson, J.P. Quinn, A.G. Marshall, B. Mukhopadhyay, J. Am. Soc. Mass Spectrom. 15 (2004) 1099.

[37] M.W. Senko, C.L. Hendrickson, L. Pasa-Tolic, J.A. Marto, F.M. White, S. Guan, A.G. Marshall, Rapid Commun. Mass Spectrom. 10 (1996) 1824.
[38] S.B. Hake, C.D. Allis, Proc Natl. Acad. Sci. USA 103 (2006) 6428.
[39] B.A. Garcia, S.A. Busby, J. Shabanowitz, D.F. Hunt, N. Mishra, J. Proteome Res. 4 (2005) 2032.
[40] M.M. Vestling, M.A. Kelly, C. Fenselau, Rapid. Commun. Mass Spectrom. 8 (1994) 786.
[41] M.M. Vestling, C. Fenselau, Anal. Chem. 66 (1994) 471.
[42] W. Fischle, B.S. Tseng, H.L. Dormann, B.M. Ueberheide, B.A. Garcia, J. Shabanowitz, D.F. Hunt, H. Funabiki, C.D. Allis, Nature 438 (2005) 1116.
[43] E. McKittrick, P.R. Gafken, K. Ahmad, S. Henikoff, Proc Natl. Acad. Sci. USA 101 (2004) 1525.
[44] S.B. Hake, B.A. Garcia, E.M. Duncan, M. Kauer, G. Dellaire, J. Shabanowitz, D.P. Bazett-Jones, C.D. Allis, D.F. Hunt, J. Biol. Chem. 281 (2006) 559.